

Structure and deformation of high-modulus alumina–zirconia fibres

X. YANG, X. HU, R. J. DAY, R. J. YOUNG

Polymer Science and Technology Group, Manchester Materials Science Centre, UMIST and University of Manchester, Manchester M1 7HS, UK

The relationship between structure and mechanical properties for high-modulus alumina–zirconia fibres PRD-166 has been examined in detail. The structure has been characterized using a combination of wide-angle X-ray diffraction and scanning and transmission electron microscopy. The fibres have been found to have a Young's modulus of at least 280 GPa and a fracture strength of up to 1.2 GPa. The deformation of the fibres has also been followed using Raman microscopy where it is found that the wave numbers of the two α -alumina Raman bands and two zirconia Raman bands shift on the application of strain. This is interpreted as being due to macroscopic stressing of the fibres leading to direct stressing of the metal oxide grains in the fibres. The possible application of this phenomenon for the investigation of the micromechanics of deformation of composites reinforced with PRD-166 fibres is discussed.

1. Introduction

Fibre PRD-166 was recently developed by Du Pont and consists of a continuous polycrystalline filament containing about 80% alumina, 20% zirconia and small quantities of yttria [1]. It has excellent mechanical and physical properties, such as high strength and modulus, with good retention of those properties after exposure to high temperature which makes the fibre a potential candidate for high-temperature applications in composites with metal or ceramic matrices. The development of the fibre was based on the desire to improve upon the mechanical properties of another metal oxide fibre known as Fibre FP [2] also manufactured by Du Pont. Fibre FP consists essentially of > 99% α -alumina but is often not successful for use in high-temperature composites because of the deterioration in mechanical properties which results from grain growth and creep at high temperature. The introduction of zirconia improves significantly the mechanical properties of the fibre at both room and elevated temperatures [2]. Lavaste *et al.* [3] reported their investigation on the strength and microstructure of PRD-166 fibres using X-ray diffraction (XRD) and electron microscopy. They found that the larger alumina grains have a tendency to be oriented with the [001] axis of the hexagonal α -alumina unit cells perpendicular to the fibre axis.

The technique of Raman microscopy has been found to be a very useful tool for the examination of the deformation of high-performance fibres such as high-modulus polymer fibres [4–9] and inorganic fibres such as carbon fibres [10] and silicon carbide fibres [11]. It has been demonstrated that well-defined Raman spectra can be obtained from these fibres and that the peaks of the Raman bands shift to lower

frequencies with the application of tensile stress or strain. The level of the shifts is dependent on the material being investigated, the band under consideration and the Young's modulus of the material. The shift of these Raman bands reflects changes in force constants due to changes in bond lengths and bond angles following macroscopic deformation. Although the structure of metal oxide fibres is different from that of the fibres described above, it is of interest to find out if the Raman technique can be used to investigate their deformation behaviour.

This present investigation is concerned first of all with the structure and tensile properties of PRD-166 fibres. It is then shown that well-defined Raman spectra can be obtained from individual fibres and that the positions of the Raman bands in the spectra are sensitive to strain. This behaviour is then correlated with the structure of the fibres.

2. Experimental procedure

2.1. Materials and characterization

The PRD-166 fibres used in this study were supplied by Du Pont and Fibre FP alumina fibres supplied by the same company were also used for comparison purposes. The details of the characterization of Fibre FP has been reported in detail by Dhingra [2].

Individual fibres were examined in a Philips EM505 scanning electron microscope (SEM) operated at 10 kV. Samples were cleaned first with ether and then with ethyl alcohol. They were then coated with a thin layer of gold in a sputter-coating unit to avoid charging in the microscope. Fracture surfaces of fibres deformed in tension were also observed in the SEM.

A transmission electron microscope (TEM) investigation was also conducted using both a Philips 301 and an analytical electron microscope, Philips 400T, equipped for energy dispersive X-ray analysis (EDX). Thin films for TEM investigation were prepared by ion-beam thinning. In order to do this, a single layer of parallel fibres was placed between two thin aluminium foils. The assembly was then heated in an oven at 560°C in an argon atmosphere to produce a composite. The composite sandwich obtained was then polished mechanically down to about 50 µm and thinned in the ion-beam thinner. Electron beam transparency was achieved using an angle of bombardment of 15° for 18 h and then 10° for 2 h to enlarge the thin area. In general, several attempts were necessary before suitable specimens could be obtained. Wide-angle X-ray scattering (WAXS) patterns were obtained from bundles of parallel fibre using a flat-plate transmission geometry and nickel-filtered CuK_α radiation from a Philips PW1010 generator.

2.2. Mechanical testing

In the present study all tests were conducted at room temperature ($21 \pm 1^\circ\text{C}$) and an Instron mechanical testing machine (model 1121) was used for the uniaxial tensile tests. A 5 N load cell was employed and measurements were made using a 0.5 N full-scale deflection with a cross-head speed of 1 mm min^{-1} . Individual PRD-166 fibres were mounted for testing using the method described in detail earlier [8] and the data were collected for the stress-strain curves using chart paper. Gauge lengths of 50, 75 and 100 mm were employed and at least 20 specimens were used for each gauge length. The diameter of the fibres was measured using an optical microscope. Measurements were made at three points on the gauge length for each specimen before deformation and the average values were used to calculate the stresses for individual fibres. Recent studies by Davis and co-workers (e.g. [12]) have shown that optical measurements of the diameters of fibres normally overestimate the value of diameter due to diffraction effects at the fibre edge. This has consequences upon the values of fibre modulus determined during mechanical testing.

2.3. Raman microscopy

A Raman microscope system was employed to obtain Raman spectra of individual PRD-166 fibres. The system is based upon a SPEX 1403 double monochromator with a charge-coupled device (CCD) camera connected to a modified Nikon optical microscope. Raman spectra were obtained by focusing the 488 nm laser beam from a 100 mW Ar^+ ion laser to a 1–2 µm diameter spot on individual fibres [8, 9].

Spectra were obtained from fibres during deformation in a small straining rig which fitted directly on to the microscope stage. Individual fibres were fixed on the rig using aluminium foil tabs and a cyanoacrylate adhesive giving a gauge length of about 20 mm which was measured accurately using the optical microscope. The fibres were extended in steps of about

0.05% or 0.1% using the micrometer attachment of the straining rig.

3. Results and discussion

3.1. Structure

The measurements using optical microscopy showed that the fibre diameter ranged between 17.78 and 20.55 µm with a mean value of $18.77 \pm 0.62 \mu\text{m}$.

Fig. 1 is a typical scanning electron micrograph of the PRD-166 fibres revealing the rough granular structure of the fibre surface with the sizes of the grains on the surface ranging from 0.1–0.75 µm. This is thought to be an advantage in making composites with the surface roughness of the fibres giving rise to good bonding between the fibres and matrix [2]. A fracture surface of the fibres is shown in Fig. 2, showing typical brittle intergranular fracture. Because of the granular appearance of the fracture surface it is difficult to detect the fracture initiation point.

Elemental analysis of the polished cross-section of a fibre was also conducted using EDX coupled with

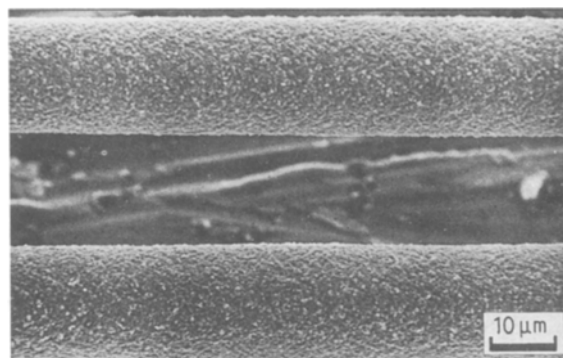


Figure 1 Scanning electron micrograph of the PRD-166 fibres.

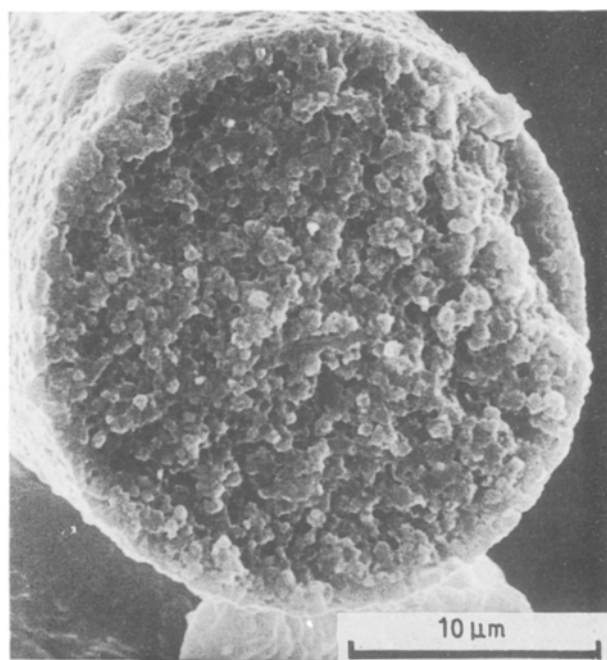


Figure 2 Scanning electron micrograph of the fractured end of a PRD-166 fibre.

scanning electron microscopy. The analysis indicated that aluminium, zirconia and yttrium were all present in the fibre and the proportional weights of their oxides is 72.7:26.1:1.3, respectively. The introduction of small quantities of yttria improves the stability of the zirconia tetragonal phase [1]. It was found, using EDX analysis from point-to-point with a 100 nm probe size, that these oxides were dispersed uniformly over the section.

A WAXS pattern of the fibres is shown in Fig. 3. This shows a pattern consisting of a set of sharp rings which can be indexed as a mixture of both α -alumina and tetragonal zirconia crystals. The pattern is consistent with a polycrystalline structure with a relatively large crystal size and a high degree of crystalline perfection in the fibres. It should be noted that there is no indication of texture in the WAXS pattern.

Transmission electron micrographs of longitudinal sections of PRD-166 fibres are shown in Fig. 4. They were obtained from both the core (Fig. 4a) and skin (Fig. 4b) regions of the section. A selected-area diffraction (SAD) pattern obtained from the core region of the fibre is also presented with the corresponding micrograph. The arrows on the micrographs indicate the direction of the fibre axis. The transmission electron micrographs indicate that the microstructure of the PRD-166 fibre is considerably different from that of polymer fibres [8, 9] and of other inorganic fibres such as silicon carbide [13, 14] and carbon fibres [15]. It appears that the PRD-166 fibres are made up of a large number of separate α -alumina and zirconia grains which were identified using EDX in the TEM. The grain size was found to be rather variable ranging from 0.1–0.6 μm for α -alumina and about 0.1 μm for zirconia. There is also a number of small particles, a few tens of nanometres in size, present in the fibres. It can be seen that the grains are in the form of regular polyhedra which appear to be randomly arranged with no preferred orientation relative to the fibre axis. This is not consistent with the findings of the WAXS

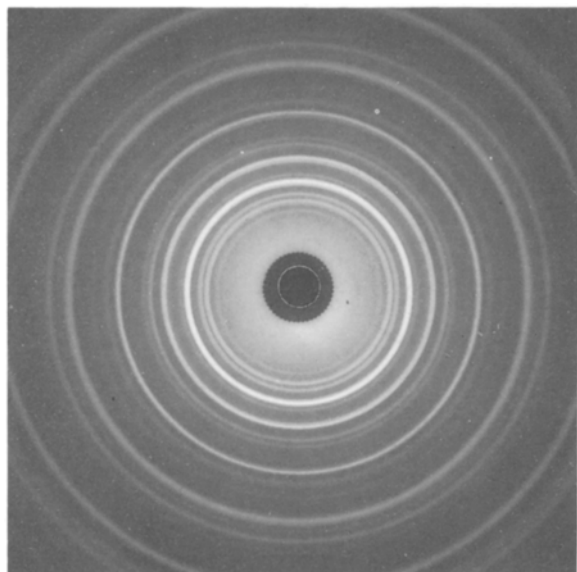


Figure 3 Wide-angle X-ray diffraction pattern obtained from the PRD-166 fibres.

study reported by Lavaste *et al.* [3] but is consistent with the WAXS patterns from this present study (Fig. 3). No structural difference was found between the core and skin regions of the fibres.

The electron diffraction pattern shown in Fig. 4a was obtained using a selected-area aperture of 1.8 μm diameter. The diffraction pattern consists of spots because most of the grains are not much smaller than the SAD aperture and so there are not enough grains in the aperture to give complete rings in the diffraction pattern. Nevertheless there appears to be no trace of any texture in the SAD pattern, again consistent with the WAXS findings.

Voids bounded by the faces of neighbouring grains such as those shown in Fig. 4a and Fig. 5 are found in both the skin and core regions of the fibres. The micrograph in Fig. 5 was obtained at relatively high magnification and shows the detailed structure of the void. The voids are clearly a potential point of initiation of failure for the fibres. However, it is not clear as to whether or not they are an inherent structural feature of the fibres or an artefact caused by the ion-beam thinning process.

3.2. Mechanical testing

The stress–strain curve for a PRD-166 fibre is presented in Fig. 6, showing a linear relationship between stress and strain. The strength obtained for the samples of 50 cm gauge length is 1180 ± 280 MPa, which is in good agreement with the value reported by Romine [1] for a similar gauge length. The Young's

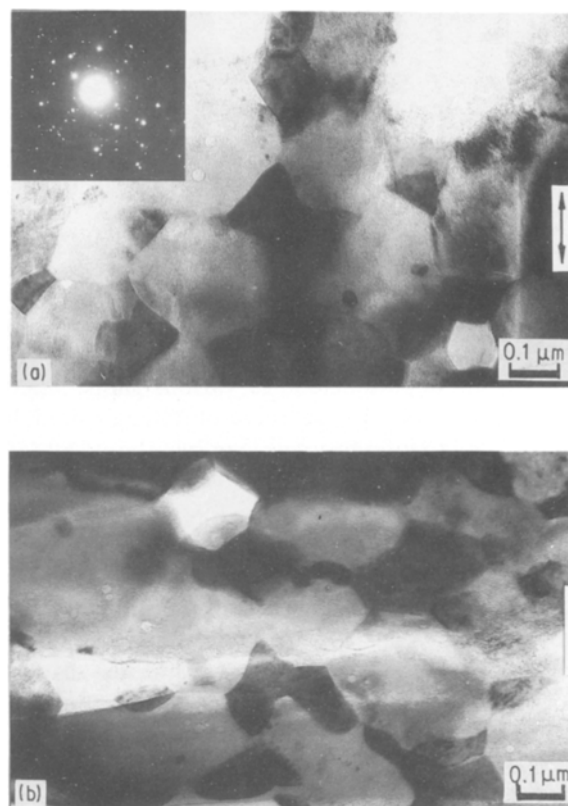


Figure 4 Transmission electron micrographs and SAD pattern (inset) obtained from the PRD-166 fibres. (a) Core. (b) Skin. The arrows indicate the direction of the fibre axis.

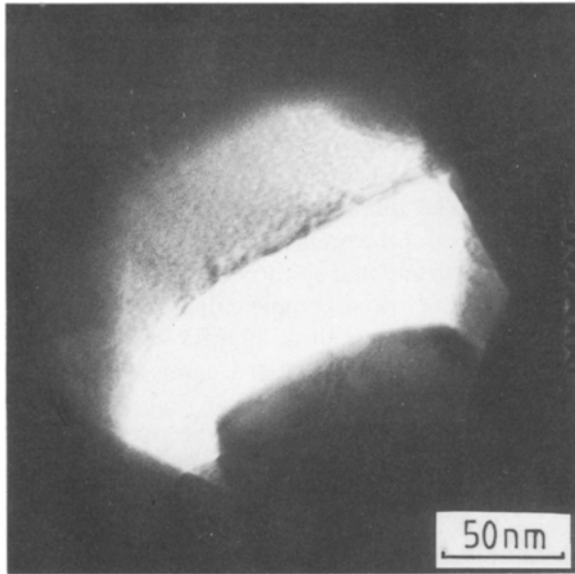


Figure 5 A typical void in the PRD-166 fibres.

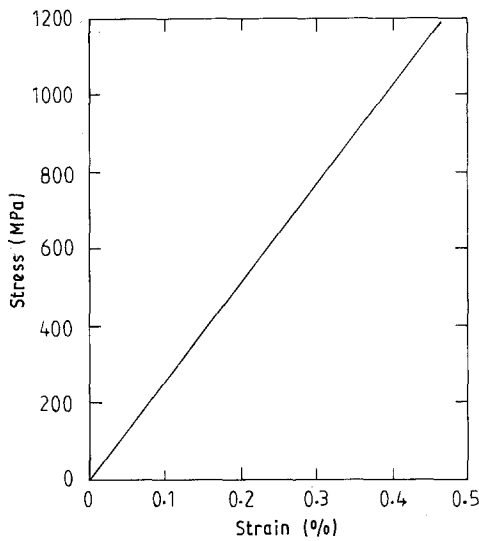


Figure 6 A typical stress-strain curve obtained for an individual PRD-166 fibre.

modulus and elongation-to-break for the same gauge length are 254 ± 12 GPa and 0.46%, respectively. The values of these parameters for various gauge lengths are given in Table I. The value of Young's modulus extrapolated to infinite gauge length is about 280 GPa which is significantly less than the value of 380 GPa quoted by Romine [1] for PRD-166. For their current production of PRD-166 fibres, Du Pont now report a value of modulus of 300–310 GPa [12]. They have also shown that machine compliance can be an important factor when determining the modulus of ceramic fibres [12]. In addition, because the diameter of our fibres may have been slightly overestimated as explained in Section 2.2, it appears that our value of 280 GPa can now be rationalized with other reported values [1, 12].

Table I shows a decrease in the values of strength and elongation to break with an increasing gauge length. This could be explained as being due to the

presence of the voids as revealed in Fig. 5 or other possible imperfections, such as the general surface roughness (Fig. 1). Recent work at Du Pont [12] has shown that there is a distribution of fibre strengths due to defects which can be analysed using a two-parameter Weibull distribution [16].

TABLE I Dependence of the mechanical properties of the PRD-166 fibres on gauge length

	Gauge length (mm)		
	50	75	100
Number of tests	21	18	19
Strength (MPa)	1180	955	840
Elongation to break (%)	0.46	0.37	0.32
Young's Modulus (GPa)	254	259	264

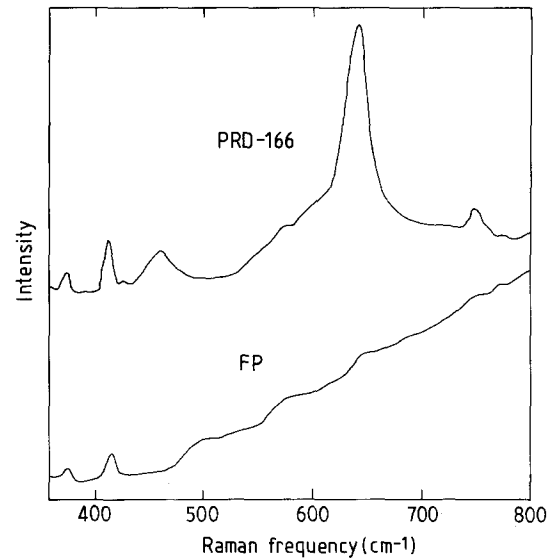


Figure 7 Raman spectra for the PRD-166 and FP fibres.

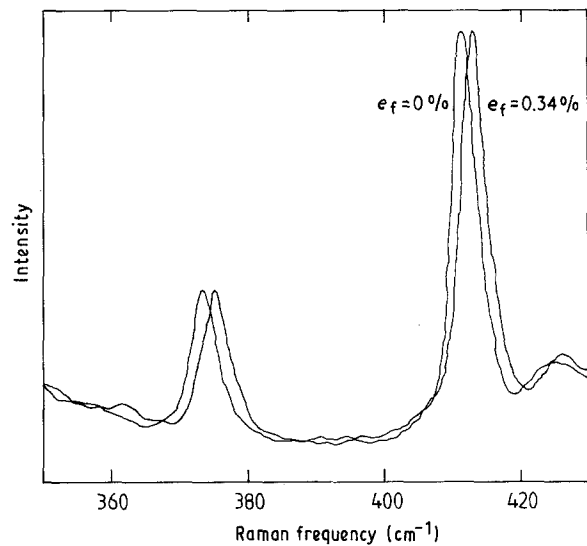


Figure 8 Shift in the positions of the 378 and 415 cm^{-1} Raman bands with strain for an individual PRD-166 fibre.

3.3. Raman microscopy

Raman spectra for the PRD-166 fibres could be obtained using a relatively low power of laser (~ 2 mW) and reasonable exposure times (~ 100 s). A typical spectrum for the fibre is shown in Fig. 7. For comparison purposes the Figure also shows the Raman spectrum for Fibre FP which is essentially pure α -alumina. It can be seen that the spectrum for the PRD-166 fibres consists of several well-defined bands between wave numbers of 360 and 800 cm^{-1} . The peak positions of the five principal bands are 378, 415, 460, 641 and 747 cm^{-1} , respectively. In contrast, the Raman spectrum for Fibre FP has only two main peaks at wave numbers of about 380 and 420 cm^{-1} , respectively. From this observation and the Raman study of alumina gels reported by Assih *et al.* [17], it

is clear that the two peaks at 378 and 415 cm^{-1} can almost certainly be assigned to the α -alumina component in the PRD-166 fibres. Recent experimental studies upon relatively pure zirconia in our laboratory [18] have indicated that the two bands at 460 and 641 cm^{-1} correspond to the zirconia component of the fibres. The band at 747 cm^{-1} is currently unassigned. It has not yet been possible to assign the Raman bands to specific molecular vibrations due to the lack of theoretical analyses. In this present study interest has been concentrated upon the effect of deformation upon the wave numbers of the five Raman bands in the PRD-166 fibres.

Fig. 8 shows the Raman spectrum for the PRD-166 fibres in the region $350\text{--}430\text{ cm}^{-1}$ in the undeformed state and following tensile deformation of the fibres to

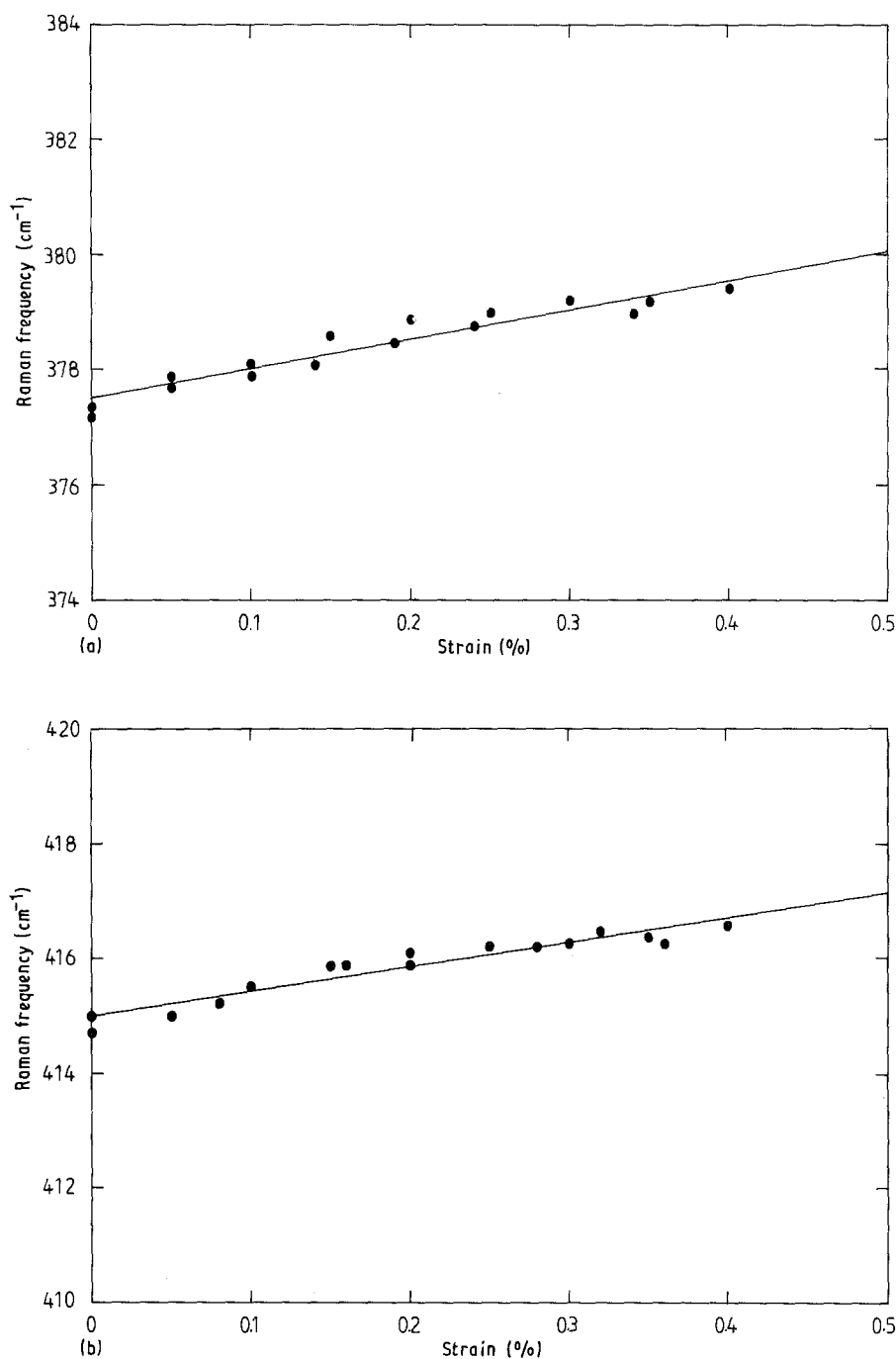
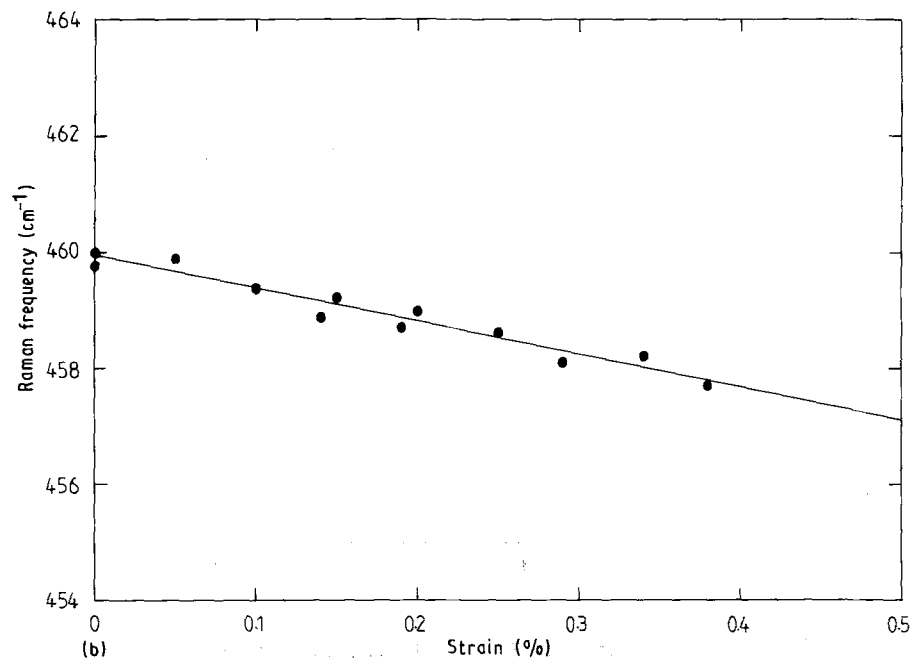
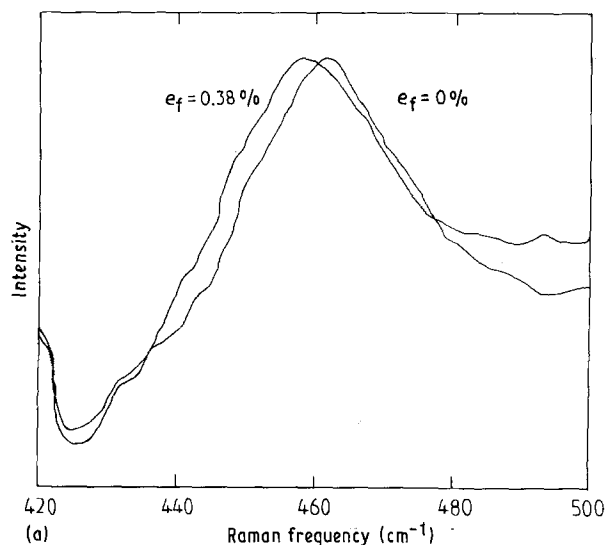


Figure 9 Dependence of the position of the Raman bands on applied strain for the PRD-166 fibres. (a) 378 cm^{-1} band. (b) 415 cm^{-1} band.

0.34% strain. It can be seen that both the 378 and 415 cm^{-1} bands shift to higher frequency with applied strain. It is worth noting that this finding is different from that for most other materials which have been investigated so far. For other high-performance fibres such as polydiacetylenes [4, 5], Kevlar [6, 7], PBT [8], PBO [9], graphite fibres [10] and silicon carbide fibres [11], it has been found that the Raman-active bands invariably shift to lower frequency with applied tensile strain. It is clear that because the PRD-166 fibres are polycrystalline, the macroscopic deformation of the fibres must occur by the deformation of the crystals in the fibres such as crystal stretching or crystal rotation. This means that the peak shift of the Raman bands with applied strain must be related directly to deformation of the crystal lattice. In order to understand this phenomenon fully a detailed theoretical study of the Raman scattering from metal oxide would have to be undertaken.

It is difficult to determine whether or not there is any broadening of the Raman bands with applied strain, which is typical of other high-modulus fibres [6–11]. This is due to the low elongation to break and relatively high fluorescence for the PRD-166 fibres



which makes any broadening difficult to detect. The effect of deformation upon the peak positions for both of the Raman bands in Fig. 8 is shown in Fig. 9. There is a linear shift in wave number with strain until fibre failure occurs and the slope of the line for the 378 cm^{-1} band is $+4.9 \text{ cm}^{-1}/\%$ strain and $+4.4 \text{ cm}^{-1}/\%$ strain for the 415 cm^{-1} band.

The effect of strain upon the peak position for the 460 cm^{-1} band due to the zirconia component of the fibres is shown in Fig. 10. It can be seen from Fig. 10a that the band shifts to lower frequency with applied strain. Also some band broadening with strain is evident even though there is relatively high fluorescence for the band. The behaviour of this band is similar to that of other fibres [4–11]. Fig. 10b shows that there is a linear relation between the Raman frequency and the strain for this 460 cm^{-1} band with a slope of $-5.7 \text{ cm}^{-1}/\%$ strain.

The strong band with a peak position at 641 cm^{-1} , which is due to zirconia, has the highest intensity of all the Raman active bands for the PRD-166 fibres. A shift of the peak with applied strain was also found for this band as shown in Fig. 11a and b. It can be seen from Fig. 11b that, in contrast to the 460 cm^{-1} band, the band shifts to higher frequency with applied strain. Hence it can be seen that different Raman bands for the same material can shift with applied tensile strain in different directions, either to higher frequency or to lower frequency. The relationship between the Raman frequency and the strain is shown in Fig. 11b revealing a linear relationship with a line slope of $+4.3 \text{ cm}^{-1}/\%$ strain. The broadening of both of the zirconia bands shows that within the fibres the zirconia grains are experiencing different levels of stress as a result of the specific microstructure of the fibres.

The Raman band at 747 cm^{-1} has the highest level of fluorescence so the data for the band are rather scattered. The preliminary examination indicated that the band shifts to lower frequency with applied tensile strain and the relation between the Raman frequency and the strain has a linear relationship with a slope of

Figure 10 (a) Shift in the position of the 460 cm^{-1} Raman band with strain for an individual PRD-166 fibre. (b) Dependence of the peak position of the 460 cm^{-1} Raman band on applied strain for the PRD-166 fibres.

– 3.7 cm⁻¹/% strain. Clearly the linear relationship between the Raman frequency and the strain for all five bands examined in the study is consistent with the linear stress–strain curve (Fig. 6) for the fibres. This shows that the strain sensitivity of the band is a reflection of the deformation at the crystal lattice level of the two metal oxide components in the fibres, due to macroscopic deformation.

Table II lists the peak positions and strain sensitivity of the five Raman active bands for the α -alumina and zirconia components in the PRD-166 fibres. It can be seen from the Table that the positions of all the Raman bands are sensitive to applied strain and the peak shift can be due to either high frequency or lower frequency depending upon the band under consideration.

Previous studies have shown that for most high-modulus fibres, Raman microscopy can be used to follow the micromechanics of deformation of both the fibres and of fibre-reinforced composites [19–25]. It appears from this present study that this approach could be extended to composites consisting of PRD-166 fibres in either a ceramic or metal matrix.

4. Conclusions

PRD-166 fibres have a granular structure with two component grains in the fibres: α -alumina grains and zirconia grains, the latter containing a very small quantity of yttria. The size of these grains ranges between 0.1 and 0.75 μm and they are found to be relatively perfect with no preferred orientation relative to the fibre axis. Many voids are found among the grains in the fibres and they are thought to be a potential point of initiation of the failure in the fibres.

Well-defined Raman spectra can be obtained from the individual fibres. The positions of the five well-defined Raman bands are all sensitive to the level of applied strain. The bands at 378 and 415 cm⁻¹ due to the α -alumina shift with strain to high frequency. Two of the Raman bands (at 460 and 747 cm⁻¹) shift to lower frequency with applied tensile strain whereas the strong 641 cm⁻¹ zirconia band shifts to higher frequency. It can be concluded that Raman microscopy is a powerful method of following the deformation of high performance metal oxide ceramic fibres.

Acknowledgements

The authors are grateful to E.I. Du Pont de Nemours for supplying the fibres and to the Science and Engineering Research Council for financial support. They also thank Dr H. A. Davis (Du Pont) for helpful comments upon the manuscript.

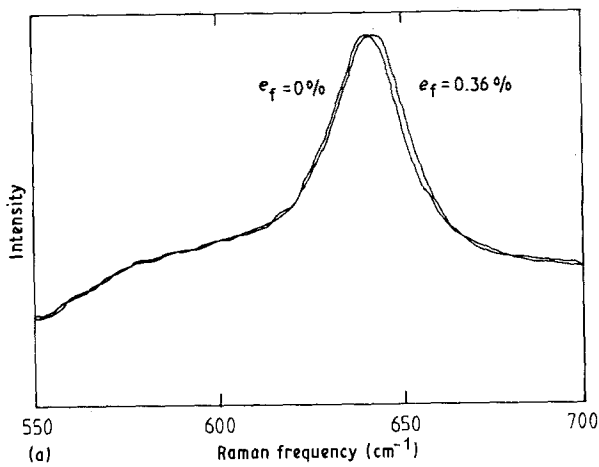


TABLE II Strain-dependent shifts for the five Raman bands in the PRD-166 fibres giving the band assignments

Band (cm ⁻¹)	$\Delta\nu$ (cm ⁻¹ /% strain)	Assignment
378	+ 4.9 ± 0.7	α -Alumina
415	+ 4.4 ± 0.8	α -Alumina
460	- 5.7 ± 0.9	Zirconia
641	+ 4.3 ± 0.8	Zirconia
747	- 3.7 ± 0.9	?

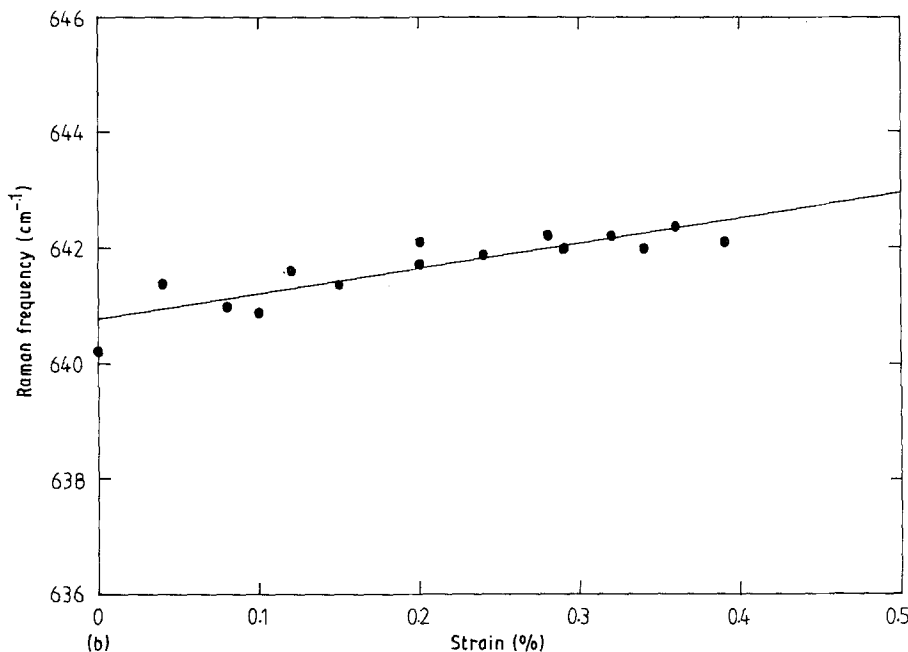


Figure 11 (a) Shift in the position of the 641 cm⁻¹ Raman band with strain for an individual PRD-166 fibre. (b) Dependence of the peak position of the 641 cm⁻¹ Raman band on applied strain for the PRD-166 fibres.

References

1. J. C. ROMINE, *Ceram. Engng Sci. Proc.* **8** (1987) 755.
2. A. K. DHINGRA, *Phil. Trans. R. Soc. Lond.* **A294** (1980) 411.
3. V. LAVASTE, M. H. BERGER and A. R. BUNSELL, in "Fourth European Conference on Composite Materials", 25–28 September 1990, Stuttgart, FRG, edited by J. Füller, G. Grüniger, K. Schutter, A. R. Bursell and A. Massiah (Elsevier Applied Science, London, 1991) p. 561.
4. D. N. BATCHELDER and D. BLOOR, *J. Polym. Sci. Polym. Phys. Ed.* **17** (1979) 569.
5. C. GALIOTIS, R. J. YOUNG and D. N. BATCHELDER, *ibid.* **21** (1983) 2483.
6. C. GALIOTIS, I. M. ROBINSON, R. J. YOUNG, B. J. E. SMITH and D. N. BATCHELDER, *Polym. Commun.* **26** (1985) 354.
7. S. VAN DER ZWAGG, M. G. NORTHOLT, R. J. YOUNG, I. M. ROBINSON, C. GALIOTIS and D. N. BATCHELDER, *ibid.* **28** (1987) 277.
8. R. J. DAY, I. M. ROBINSON, M. ZAKIKHANI and R. J. YOUNG, *Polymer* **28** (1987) 1833.
9. R. J. YOUNG, R. J. DAY and M. ZAKIKHANI, *J. Mater. Sci.* **25** (1990) 127.
10. I. M. ROBINSON, M. ZAKIKHANI, R. J. DAY, R. J. YOUNG and C. GALIOTIS, *J. Mater. Sci. Lett.* **6** (1987) 1212.
11. R. J. DAY, V. PIDDOCK, R. TAYLOR, R. J. YOUNG and M. ZAKIKHANI, *J. Mater. Sci.* **24** (1989) 2898.
12. C. A. LUNDGREN, H. A. DAVIS, C. R. NEAL and P. H. SCHMITZ, in "Proceedings of International Conference of Fibre and Textile Science", Institute of Textile Science, Ottawa, Canada, April 1991, pp. 105–110.
13. S. R. NUTT and F. E. WAWNER, *J. Mater. Sci.* **20** (1985) 1953.
14. X. YANG and R. J. YOUNG, unpublished results, 1991.
15. D. J. JOHNSON, in "Applied Fibre Science", Vol. 3, edited by F. Happey (Academic Press, 1979) p. 152.
16. W. J. WEIBULL, *J. Appl. Mech.* **18** (1951) 293.
17. T. ASSHIH, A. AYRAL, M. ABENOZA and J. PHALIPPON, *J. Mater. Sci.* **23** (1988) 3326.
18. R. J. YOUNG and X. HU, unpublished results, 1990.
19. C. GALIOTIS, R. J. YOUNG, P. H. J. YEUNG and D. N. BATCHELDER, *J. Mater. Sci.* **19** (1984) 3640.
20. I. M. ROBINSON, R. J. YOUNG, C. GALIOTIS and D. N. BATCHELDER, *ibid.* **22** (1987) 3642.
21. C. GALIOTIS, I. M. ROBINSON, D. N. BATCHELDER and R. J. YOUNG, in "Engineering Applications of New Composites", edited by S. A. Paipetis and G. C. Papanicolaou (Omega Scientific, Wallingford, 1988) p. 409.
22. R. J. YOUNG, R. J. DAY, M. ZAKIKHANI and I. M. ROBINSON, *Comp. Sci. Tech.* **34** (1989) 243.
23. C. GALIOTIS, J. A. PEACOCK, D. N. BATCHELDER and I. M. ROBINSON, *Composites* **19** (1988) 321.
24. R. J. YOUNG and P. P. ANG, in "Fourth European Conference on Composite Materials", 25–28 September 1990, Stuttgart, FRG, edited by J. Füller, G. Grüniger, K. Schutter, A. R. Bursell and A. Massiah (Elsevier Applied Science, London, 1991) p. 685.
25. C. GALIOTIS and H. JAHANKHANI, *ibid.*, p. 679.

*Received 22 April
and accepted 1 May 1991*